Two-Photon Fluorescence Correlation Spectroscopy: Method and Application to the Intracellular Environment

Keith M. Berland, Peter T. C. So, and Enrico Gratton

Laboratory for Fluorescence Dynamics, Department of Physics, University of Illinois at Urbana-Champaign, Urbana, Illinois 61801 USA

ABSTRACT   We report on the application of two photon molecular excitation to fluorescence correlation spectroscopy. We demonstrate the first fluorescence correlation spectroscopy measurements of translational mobility in the cytoplasm of living cells. Two-photon excitation inherently excites small sample volumes in three dimensions, providing depth discrimination similar to confocal microscopy, without emission pinholes. We demonstrated accurate measurements of the diffusion constant, D, for particles of several different known sizes, in bulk solutions of different viscosity. We then showed measurements of translational diffusion for 7- and 15-nm radius latex beads in the cytoplasm of mouse fibroblast cells. We measured time-dependent diffusion coefficients. When first injected in the cells, the spheres moved from two to five times slower than in water, with average rates of 18×10^{-8} cm^2/s for the 7 nm and 5×10^{-8} cm^2/s for the 15 nm radius spheres. After a few hours, spheres stick to the cells, and the motion slows down 10 to 100 times.

INTRODUCTION

Since its introduction more than 20 years ago, fluorescence correlation spectroscopy (FCS) has had proposed applications in many fields of biophysical investigation (Elson and Magde, 1974; Elson et al., 1974). Fluorescence fluctuation is an attractive method because of the high sensitivity and spectral selectivity one can achieve with fluorescence measurements. With optimized optical systems, one can detect single molecules (Eigen and Rigler, 1994; Rigler et al., 1992). FCS has been applied to measuring translational diffusion, rotational diffusion, flow, and chemical reactions (Elson and Magde, 1974; Elson et al., 1974; Magde et al., 1978; Elson, 1985; Icenogle and Elson, 1983a, b). Applications have been proposed in membrane dynamics, polymer dynamics, and many other areas (Icenogle and Elson, 1983; Fahey and Webb, 1978; Borejdo, 1979). Much work has also been done to realize the FCS potential of monitoring aggregation, with both scanning correlation methods and high order correlation analysis (Weissman et al., 1976; Palmer and Thompson, 1987; Petersen, 1986; Meyer and Schindler, 1988; Petersen, 1984; Qian and Elson, 1990; Koppel et al., 1994). Due to various experimental difficulties, however, it is not a widely used technique. The basic problem is that experimentally measurable fluctuations in fluorescence intensity occur only for very small sample volumes. For one-photon molecular excitation, lasers can be focused to sub-micron beam waists in the radial dimensions, but there is no confinement along the beam axis (z axis). Thus, most early applications were limited to two-dimensional systems, such as diffusion of labeled proteins or lipid probes in membranes

(see above references). Another possibility was to use very thin sample holders in order to confine the sample (volume) along the z axis. In any case, there was no possibility to do FCS measurements inside of live, intact cells.

In recent years, the application of confocal microscopy techniques to FCS has successfully solved the volume problem and made possible measurements of diffusion in bulk (three dimensional, 3D) samples (Qian and Elson, 1991; Rigler et al., 1993; Koppel et al., 1994). However, confocal FCS has not been applied to the study of diffusion inside cells. An alternative method to solve the 3D volume problem is to use two-photon excitation, which excites only a small defined sub-volume of a bulk sample. This allows us to do FCS in bulk solutions, as in confocal techniques. There are additional benefits associated with two-photon excitation which will be discussed below, where we demonstrate the possibility to perform fluctuation measurements inside of live cells.

Research on the transport properties and hydrodynamic conditions of cellular environments is a very active area of biophysical research (Luby-Phelps, 1994). FCS and photobleaching techniques and, more recently, single particle tracking experiments have all been used to study diffusion and transport on membrane surfaces. At present, there are only a limited number of techniques capable of probing intracellular diffusion. Fluorescence photobleaching (FPR/FRAP) is the most widely used, and many authors have investigated transport properties in the cytoplasm in some detail. Single particle tracking is also becoming a very popular method, and has recently been introduced as a 3D method (Kao and Verkman, 1994). Our interest is in providing an alternative method to probe the environment inside of living cells. FCS and FRAP experiments can complement each other well. There are some important differences in the methods, and thus comparing results may prove valuable. First, FCS is generally useful for very low probe concentrations, while FRAP experiments can be done with higher probe concentrations. Also, FRAP experiments are done by perturbing

the system away from equilibrium. It is not unreasonable to suppose that cellular transport may not always be linear with probe concentration, or that bleaching may in some instances introduce artifacts. Another important difference involves the 3D resolution of each method. Two-photon FCS has true 3D resolution, while most FRAP instruments use one-photon excitation. Single photon excitation bleaches through the entire cell, without z direction localization. It is possible to do two-photon photobleaching recovery to get the same 3D resolution (Piston et al., 1992). True 3D measurements may allow construction of a 3D diffusion map of a cell. Finally, others have demonstrated the FCS potential to monitor aggregation, rotations, and chemical reactions. Perhaps with some work this can be done inside of a cell. In any case, it is clear that two-photon FCS experiments may prove valuable in studying cellular interiors.

TWO-PHOTON EXCITATION

Two-photon excitation is the simultaneous absorption of two photons; their energies sum to the energy of the transition. Thus, for example, one can excite the ultraviolet 390-nm transition with two red 780-nm photons. The use of two-photon excitation for biological applications in microscopy was first proposed by Denk et al. (1990). For a general discussion see Friedrich (1982). Two-photon excitation is a nonlinear absorption process, and the excited fluorescence intensity is proportional to the square of the exciting laser intensity. For a system with probe concentration $C(\vec{r},t)$ and laser intensity $I(\vec{r},t)$, we will observe fluorescence intensity,

$$F(t) \approx \alpha \int dV I^2(\vec{r}, t) C(\vec{r}, t), \quad (1)$$

where $\vec{r} = (r, z) = (x, y, z)$ and the integral is over all space. The constant α accounts for the absorption cross-section, quantum yield, and light collection efficiency. Fig. 1 confirms the intensity squared dependence of the excitation process. This measurement of fluorescence intensity as a function of laser power was made using a concentrated solution of POPOP in ethanol, using neutral density filters to vary the excitation laser power.

The main advantage of two-photon fluorescence excitation for FCS is its inherent sectioning effect of exciting only very small volumes of a bulk sample. Because two-photon absorption cross-sections are generally very small, there is only appreciable fluorescence excitation very near the focal plane of the focused laser, where the instantaneous photon flux is highest. To figure out the size and shape of the two-photon excited sample volume, we must simply evaluate the expression in Eq. 1, using some model for the intensity distribution of a focused laser. We expect a diffraction limited spot with a beam waist the size of the Airy disk. Other papers describing 3D FCS and FRAP (confocal) have modeled the intensity with a "quasi-cylindrical" (Gaussian in three directions) volume. We can also fit our data using this model. In this case either the diffusion coefficient or beam waist may correspond to the theoretically expected value, but not both.
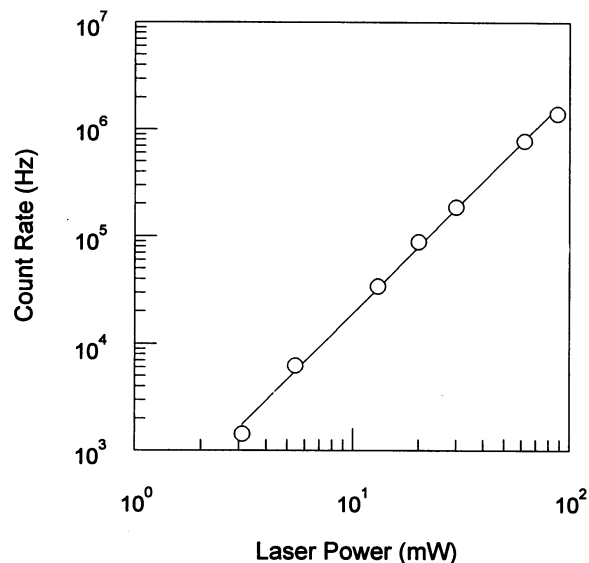

FIGURE 1 Fluorescence intensity as a function of excitation power. When data is fit to the form $y = ax^b$ we recover $b = 2.04$.

In contrast, we found that both the recovered diffusion coefficient and beam waist agree with the theoretically expected values when we use the Gaussian-Lorentzian form of the intensity

$$I(r, z) = \frac{2I_0 w_0^2}{\pi w^2(z)} \exp\left(- \frac{2r^2}{w^2(z)} \right), \quad (2)$$

where

$$w^2(z) = w_0^2\left(1 + \left(\frac{z}{z_R}\right)^2\right) \quad \text{and} \quad z_R = \frac{\pi w_0^2}{\lambda}. \quad (3)$$

Fig. 2 A is a plot of this intensity distribution for a focused laser beam. The excitation profile (excited sample volume) for two-photon excitation (intensity squared) is shown in Fig. 2 B. It is easy to see the optical z sectioning effect of this method, which excites a volume of less than 1 μm^3 (10^{-15} l).

There are other benefits of using two-photon excitation which can greatly aid the measurement. Perhaps the most important is that light is absorbed only at the focal spot, thus there is no damage anywhere else in the sample. This is in contrast to confocal techniques where light is absorbed throughout the sample, and the depth discrimination is achieved using emission pinholes. Since cells are quite susceptible to photodamage, this can be a very important advantage. A second advantage is the improved rejection at the detector of scattered laser light. For two-photon excitation, the fluorescence is far removed from the excitation. For example, 720-nm light will excite a 360-nm transition. The emission range will of course depend on the specific probe used, but fluorescence from 360-nm excitation should generally fall in the range between 360 and 600 nm. Thus, it is easy to find filters that will transmit the fluorescence very efficiently and have optical densities of several decades or more in the far red.
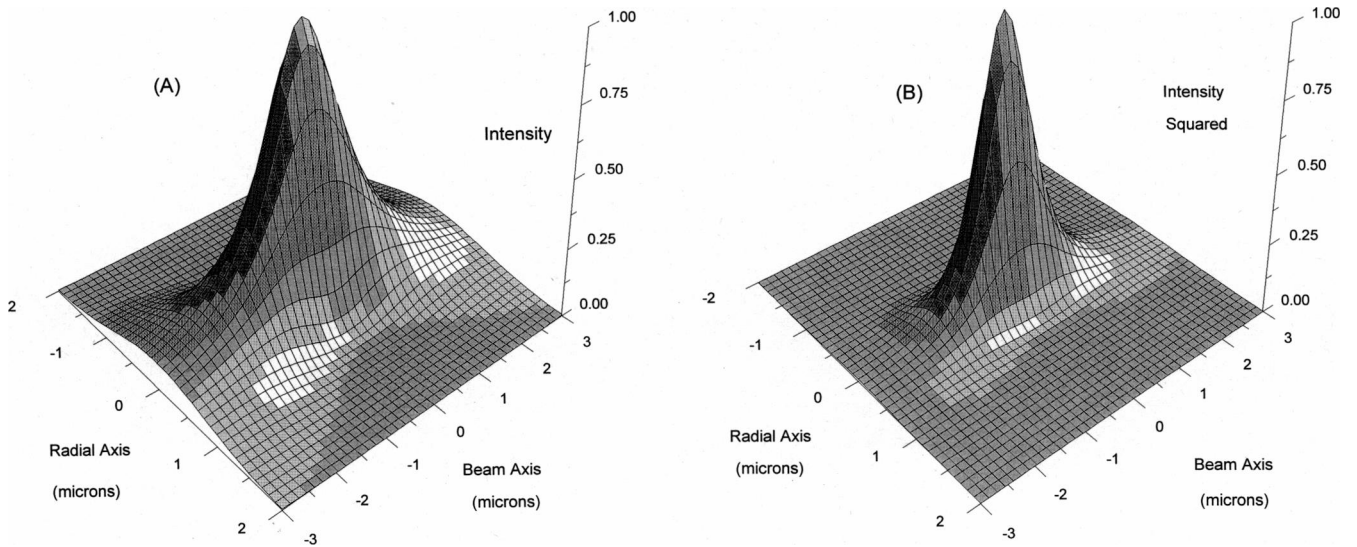
FIGURE 2   (A) Intensity distribution of a focused laser beam for the Gaussian-Lorentzian form shown in Eqs. 2 and 3 with a beam waist $w_0 = 0.5$ μm. (B) The distribution of fluorescence intensity, which is the square of the distribution in A. The sub-volume selection is quite apparent.

THEORY

For a useful review of FCS theory and measurements, see Thompson (1991). The basic principle is to measure the autocorrelation function, $G(\tau)$, of the fluorescence intensity. The fluorescence serves as a monitor of the number of particles in the volume of interest. The fluorescence intensity will fluctuate spontaneously about its equilibrium value, and the autocorrelation function contains information on the average amplitude and duration of the intensity fluctuations. The intensity fluctuations will result from number fluctuations of the fluorescent species in the volume of interest. In this paper we will consider fluctuations caused only by Brownian diffusion in and out of the volume (translational diffusion). For this case, the decay rate of the fluorescence autocorrelation function, $G(\tau)$, depends only on the diffusion coefficient for the system and the size of the excited volume. The amplitude of $G(\tau)$ depends on the number of diffusing chromophores in the excited volume. Since fluctuations occur spontaneously in any equilibrium system, FCS measurements can be performed without applying external perturbations to the sample.

Experimentally, the fluorescence intensity is measured using a photomultiplier tube for photon counting. To set up an experiment, one must choose an appropriate time scale, Δt, to monitor fluctuations, determined by the diffusion coefficient, D, and the size of the volume. A dedicated autocorrelator records the number of photon counts, $F(t)$, received in each time interval, Δt, and then calculates the autocorrelation function, $G(\tau)$ (not normalized), using the equation

$$G(\tau) \equiv \langle F(t)F(t + \tau) \rangle$$
$$= \sum_n F(n \times \Delta t) \times F((n \times \Delta t) + \tau). \tag{4}$$

The angular brackets represent a time average. This summation is done for some number of channels, N. The summation is done enough times to get sufficient signal for analysis.

MATHEMATICAL FORM FOR $G(\tau)$

The autocorrelation function defined in Eq. 4 may be rewritten as

$$G(\tau) = \langle \delta F(t)\delta F(t + \tau) \rangle + \langle F \rangle^2 \tag{5}$$

with fluctuations about the average total fluorescence intensity

$$\delta F(t) = F(t) - \langle F \rangle = \alpha \int dV I^2(\vec{r}, t)\delta C(\vec{r}, t), \tag{6}$$

due to spontaneous concentration fluctuations of the species of interest

$$\delta C(\vec{r}, t) = C(\vec{r}, t) - \langle C \rangle. \tag{7}$$

For constant laser intensity, the fluorescence intensity fluctuations will be an effective measure of the spontaneous local fluctuations about the equilibrium concentration of the fluorescent species studied. We verified that the laser intensity was sufficiently constant by measuring the correlation from a highly concentrated POPOP solution at many time scales. Since the autocorrelation measured from this sample was flat for all time scales in this study, we know correlations measured with other samples are due to concentration fluctuations and not correlated laser noise. Using Eqs. 1–3, one obtains

$$\langle F \rangle = \frac{\alpha I_0^2 w_0^4 \pi}{\lambda} \langle C \rangle. \tag{8}$$

This term simply contributes a flat background to the signal. The fluctuation term $\langle \sigma F(t)\sigma F(t + \tau)\rangle$ is more difficult to evaluate. Though the average concentration is known, the fluctuations $\delta C(\vec{r}, t)$ will have characteristic behavior governed by the diffusion equation. To solve for $G(\tau)$, we must therefore solve the diffusion equation for $\delta C(\vec{r}, t)$

$$\frac{\partial \delta C(\vec{r}, t)}{\partial t} = D\nabla^2 \delta C(\vec{r}, t). \quad (9)$$

For translational diffusion in three dimensions, it has been shown that (Thompson, 1991)

$$\langle \delta C(\vec{r}, t) \cdot \delta C(\vec{r}, t + \tau)\rangle \quad (10)$$
$$= \langle C\rangle(4\pi D\tau)^{-3/2}\exp(-|\vec{r} - \vec{r}'|^2/4D\tau).$$

D is the diffusion coefficient for the particle of interest, which we expect will follow the Stokes-Einstein equation for a spherical particle of radius R, in solution of viscosity η, at temperature T

$$D = \frac{kT}{6\pi\eta R}. \quad (11)$$

Using Eqs. 5, 6, and 10, we can write

$$\langle \delta F(\vec{r}, t)\delta F(\vec{r}', t + \tau)\rangle \quad (12)$$
$$= \alpha^2 \int d\vec{r} \int d\vec{r}' I^2(\vec{r}, t)I^2(\vec{r}', t)\langle \delta C(\vec{r}, t)\,\delta C(\vec{r}', t + \tau)\rangle.$$

This integral has no analytical form, so we report the integral form used to numerically fit our data.

$$\langle \delta F(\vec{r}, t)\delta F(\vec{r}', t + \tau)\rangle = \frac{2\alpha^2 I_0^4 w_0^6}{\lambda^2(4\pi D\tau)^{1/2}}\langle C\rangle g(D, \tau) \quad (13)$$

where

$$g(D, \tau) = \int db \, \frac{\exp(-z_R^2 b^2/2D\tau)}{b^4 + \left(2 + \dfrac{16D\tau}{w_o^2}\right)b^2 + \dfrac{1}{4}\left(\dfrac{16D\tau}{w_0^2}\right)^2}$$

$$\times \left[\frac{2b^2 + \dfrac{16D\tau}{w_0^2} - 4}{\sqrt{2}(2 + b^2)} + \frac{2}{\left(2 + b^2 + \dfrac{16D\tau}{w_0^2}\right)^{1/2}}\right] \quad (14)$$

MATERIALS AND METHODS

Fig. 3 shows the experimental setup for the two-photon FCS measurements. Our laser system is a MIRA 900 mode-locked (80 MHz) Ti:sapphire laser pumped by an Innova 410 argon ion laser (Coherent, Palo Alto, CA). High local instantaneous power (photon flux) is necessary to get significant two-photon excitation (Denk, 1990). The MIRA laser pulses are 150 fs FWHM, thus even at modest average power levels, the instantaneous power is quite high, and there is appreciable two-photon excitation probability at a focal spot. The laser power at the sample was generally between 0.1 and 50 mW. We used less than 10 mW at the sample for cell studies. For all samples considered in these studies, the correlator time bin was 0.1 ms or longer. This means there were at least 8000 laser pulses for each bin time. The high
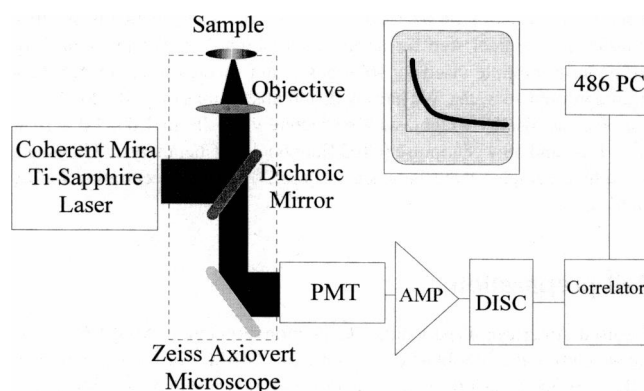

FIGURE 3 Schematic of the two-photon FCS apparatus. PMT, Hamamatsu photomultiplier tube. Amp/Disc, Pacific AD6 amplifier and discriminator. The correlators were the Nicomp 4-bit digital autocorrelator, and the BI9000AT correlator card from Brookhaven Instruments.

repetition rate is important, since it eliminates any correlation at the time scales of interest due to the laser pulses. In fact, the 80 MHz is sufficiently fast for most systems one would consider studying using FCS. We operate the laser at two wavelength regions, 780 nm to excite the absorption at 390 nm, and 960 nm to excite at 480 nm.

The apparatus is based around a Zeiss Axiovert 35 microscope (Thornwood, NY). The laser enters through the rear port of the microscope where we mounted a 50-mm focal length eyepiece lens to focus the beam at the field aperture. Upon passing through this aperture, the beam is recollimated by the tube lens inside the Axiovert. Laser light is then reflected by the low pass Chroma Technology dichroic mirror (Brattleboro, VT), and focused on the sample with a Zeiss 100X CP Achromat objective lens (N.A. = 1.25). When the laser beam reaches the objective it is expanded about 10 times. Its profile is still Gaussian, but rather flat (approaching a plane wave). We have two separate dichroics for transmission at 350–620 nm and 400–800 nm, which reflect the near infrared (IR) laser excitation. Fluorescence emission collected by the objective passes through the dichroic and a series of short pass filters to eliminate any red light reflected toward the PMT. At 380 nm, a home-built liquid filter with copper sulfate in water seems to work best, passing 80–90% of the blue and attenuating the red with an optical density of 20. We have also used a stack of four Corion short pass (500/550 nm) interference filters (Holliston, MA). These filters also work well, but the many surfaces cut more blue and pass more red light than the liquid filter. At 480 nm, we used the same liquid filter filled with Exciton IRA 980 absorber dye in methanol (Dayton, OH). Our detector was the Hamamatsu R1104 photomultiplier tube. The tube was cooled to −60° Celsius to lower dark noise. Average dark count levels were about 20 counts/s. The output of the photomultiplier tube was amplified and passed through a Pacific AD6 discriminator (Concord, CA) and sent to the correlator. For the experiments on spheres in bulk solution we used a Nicomp four-bit digital autocorrelator. For the cell studies, we used the Brookhaven Instruments Corp. BI9000AT correlator card on loan for testing (Holtsville, New York). After collection, data were transferred to a 486 personal computer for analysis using the LFD Globals Unlimited software (Urbana, IL).

Sample preparation

Clean samples are critical to do FCS measurements, since experiments are typically done at very low concentrations (nanomolar). Any aggregates and fluorescent dust contaminates not eliminated will make up an appreciable fraction of the signal, obscuring correlations due to the species of interest. All samples were held on hanging drop glass microscope slides with 1-mm wells using 0.17-mm-thick square coverslips. Before use, all slides were washed with 100% nitric acid and then rinsed with sterile water filtered using 0.2-μm Acrodisk syringe filters (Ann Arbor, MI). Sphere samples were Molecular Probes (Eugene, OR) blue fluorescence-labeled carboxylated latex fluospheres. Spheres were sonicated for 10 min before dilution to appropriate concentrations in filtered water. After dilution, spheres were filtered with 0.2-μm Acrodisk filters for the 7 nm and the 46.5 nm radius

spheres, and 1.2 μm filters for the 141 nm and 208 nm radius spheres. Filtering is a critical step for accurate measurements. For the studies of diffusion in multiple viscosity solutions, 7-nm spheres were filtered, then diluted in sucrose water. We had six different solutions of 0, 10, 20, 30, 50, and 60% sucrose by weight, with respective viscosity of 1.00, 1.33, 1.94, 3.18, 15.4, and 58.4 centipoise (CRC Handbook of Chemistry and Physics). All sphere samples were between 20 and 200 nM concentration before filtering.

Cell preparation

We used American Type Culture Collection (Rockville, MD) CRL 1503 mouse embryonic fibroblast cells grown in DMEM. For each experiment, cells were first trypsinized and spun down (1000 rpm) to pellets containing ~1,000,000 cells. They were washed by resuspending in DMEM and spun down. The pellet was then resuspended in electroporation buffer containing one size of yellow-green fluorescent spheres. The concentration of spheres in the electroporation buffer was 200 nM for the 7 nm radius spheres, and 1 μM for the larger 15-nm beads. Actually, the spheres go into the cells quite efficiently, and thus these concentrations are not far from those we use for FCS measurements in bulk solution. Samples were electroporated with a single 30-μs pulse of 300 V using the Biotechnologies and Experimental Research Inc. Electro Cell Manipulator 200 (San Diego, CA). After sitting for 10 min, cells were diluted in more growth media to wash, spun down, and the pellet resuspended in 300 μl of media. We then used this final solution of sphere loaded cells for FCS measurements, using the well slides, and allowing the fibroblast cells to settle on the coverslips of the inverted slides.

Calibration

The size of the excited sample region is affected by small variations in optical alignment and must be calibrated each time the system is aligned. The parameters in the variable part of the autocorrelation function are the beam waist w_0 and the diffusion coefficient D. Thus, we measured $G(\tau)$ for a known size particle and fit the data using a fixed value of the diffusion constant given by Stokes-Einstein, Eq. 11, to calibrate for the beam waist. This waist, w_0, was then used to fit all the data taken with a particular alignment. We used the 7-nm radius spheres ($D = 31.4 \times 10^{-8}$ cm^2/s) diffusing in water at 25°C to calibrate the instrument. For multiple data sets we find an average w_0 of 0.6 μm, which is very close to the expected value for a diffraction limited focus of 780-nm light. Data were fit using Eqs. 13 and 14 with the nonlinear least squares minimization routines of the Global Analysis software.

RESULTS

Fig. 4 shows a typical measurement of the correlation function, $G(\tau)$, for the diffusion of the 7-nm spheres in water. The necessary integration time depends on the diffusion coefficient, the brightness of the probe, and the desired accuracy for the measurement. It is possible to measure diffusion coefficients with 10–20% accuracy in a few seconds. During the measurement shown, we wanted accuracy of a few percent, thus we integrated for ~10 min.

The diffusion coefficient of a spherical particle in solution is determined by its radius, the viscosity of the solution, and the temperature, as shown in Eq. 11. To demonstrate the accuracy of our technique, we show that measurements of D for different known size spheres in water scale as expected by the Stokes-Einstein equation. We measured the diffusion coefficient for spheres of 7, 46.5, 141, and 208-nm radius in bulk water samples. Fig. 5 shows the measured values for the
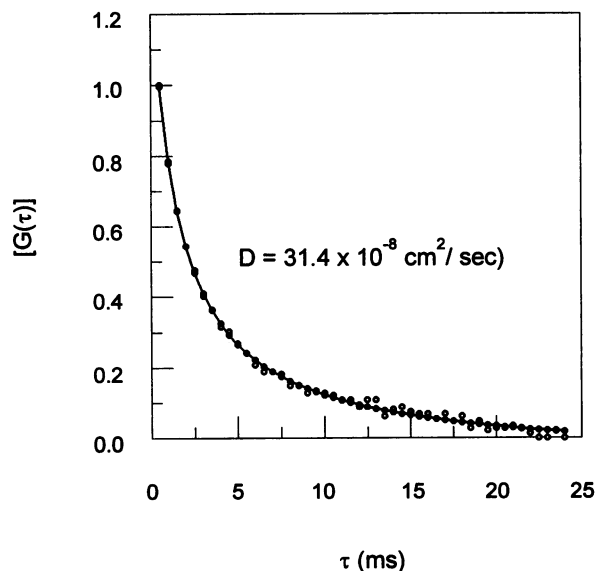

FIGURE 4   Measurement of $G(\tau)$ for fluorescent spheres of 7 nm radius in water at 22°C. $[G(\tau)]$ is the normalized $G(\tau)$ with the flat background subtracted. The diffusion coefficient is $D = 31.4 \times 10^{-8}$ cm^2/s, and the recovered beam waist was 0.56 μm. The curve is the best fit of Eqs. 13 and 14 using the fitting routines of GLOBALS Unlimited software.
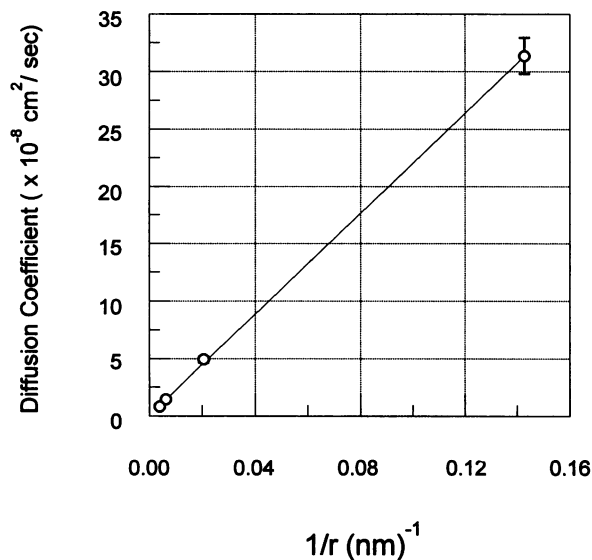

FIGURE 5   The measured diffusion coefficients for blue fluorescent spheres of 7, 46.5, 141, and 208 nm radius in water at 22°C. The line represents the diffusion coefficient expected according to Eq. 11. The beam waist was recovered by fitting the measured $G(\tau)$ for the 7-nm spheres with a fixed value of D given by the Stokes-Einstein relation. The diffusion coefficient was then measured for the other size spheres by fixing the beam waist at this recovered value and fitting for D. In some cases, the error bars are not shown since they are smaller than the plotted points.

diffusion coefficient of each size sphere plotted against one over the particle radius. All the measured values scale as expected according to the theory.

As an additional check of the accuracy, we have measured D for 7-nm spheres in sucrose-water solutions of viscosity 1,

1.33, 1.94, 3.18, 15.4, and 58.4 centipoise. Fig. 6 shows the measured values plotted against one over the solution viscosity. The measured values correspond to the expected coefficients within a few percent. These measurements demonstrate that we can accurately recover the 3D diffusion coefficients in homogeneous solution using the two-photon FCS measurement.

Cellular diffusion

Finally and most importantly, we demonstrate the possibility to perform FCS measurements inside of mouse fibroblast cells. We show measurements of the autocorrelation functions for diffusion of fluorescein-labeled carboxylated latex beads of 7 nm and 15 nm radius in the cytoplasm of the cells. The setup of the instrument was the same as described above. These measurements were made with the laser tuned to 960 nm. Working at 960 nm (480-nm excitation) is somewhat better than 780 nm, since the autofluorescence is significantly less at the longer wavelength.

We measured the diffusion coefficient for each size sphere in many cells. There are significant variations in the measured diffusion rates, depending mostly on the time lapsed after injection, but also on characteristics of individual cells and cell regions. Fig. 7 shows the autocorrelation for measurements of D with both 7- and 15-nm spheres in the cytoplasm of different cells. When the 7-nm beads were first injected in the cells (within 1.5 h), we found an average D of 18×10^{-8} cm^2/s, just over half the rate in water. This value varied by a factor of 2 in either direction between cells. We measured a slower rate for the larger 15-nm beads when first injected. The average value was 5×10^{-8} cm^2/s. Again, this

varied from cell to cell by up to 50%. We have performed control experiments by measuring the autocorrelation of the autofluorescence from cells not injected with spheres. The lack of correlations for these cells assures that our measurements were of sphere diffusion as expected. The range of measured values seems consistent with results of previous studies, which have found both that the "viscosity" in the cytoplasm is not very different from water, and that intracellular diffusion rates are often mediated by binding of the probe to cellular components (Kao et al., 1993; Bicknese et al., 1993; Luby-Phelps et al., 1986, 1993). The latex spheres are highly charged, and it is certainly not surprising that at least some binding to cell components will occur.

In fact, one phenomena we observed is that as time passes after electroporation, the measured value of the diffusion coefficient becomes slower. A few hours (2.5 or more) after electroporation we measured much slower diffusion rates. After this slow down, both size spheres move at the same range of rates, from 2×10^{-8} cm^2/s and slower. This phenomena has previously been observed (Kao and Verkman, 1994). We believe that some combination of biological changes in the cell and the binding of spheres to cell components is responsible. We speculate that the slower rates are governed by either the size of components that the spheres bind to or by some transport property of the cells. Many researchers have previously demonstrated that microinjected probes are actively transported by cells (Beckerle, 1984; Wadsworth, 1987; De Brabander et al., 1989). The rates we measured after the slow down are consistent with this possibility. It is possible to use FCS to discern active transport (or flow) from diffusive transport, though for the very slow rates in question here, FCS is much less effective than the particle tracking techniques, and we have not attempted to investigate this motion in detail. Changes in the cytoarchitecture may also contribute to the slower movement. The cells had not spread again on the coverslips at the time of our measurements. Whether or not the slowing we observed was related to the cells recovery and preparation to spread again raises an interesting possibility for future studies.

We are currently working on more cellular studies. There are two exciting possibilities guiding the direction of future work. The first is a result of our ability to measure a localized 3D diffusion coefficient, point by point. As we scan this point across (and through) the cell, we hope to reconstruct a diffusion map of all or part of a cell. The size of the region we can map out depends on the data acquisition time per point. We must improve our measurement time scale to scan a significant volume of the cell. Based on reports of other FCS researchers, we believe it is possible to shorten the acquisition time to acquire such a diffusion map. The second interesting possibility we see for two-photon cellular FCS is to continue the present work with new probes in addition to the spheres; dextrans, labeled proteins, and dye molecules are some possibilities. Comparing the motions of multiple size probes in the cells, with varying degrees of reactivity with the cell, will perhaps provide other insight into molecular transport within the cells. In fact, many of the possible probes
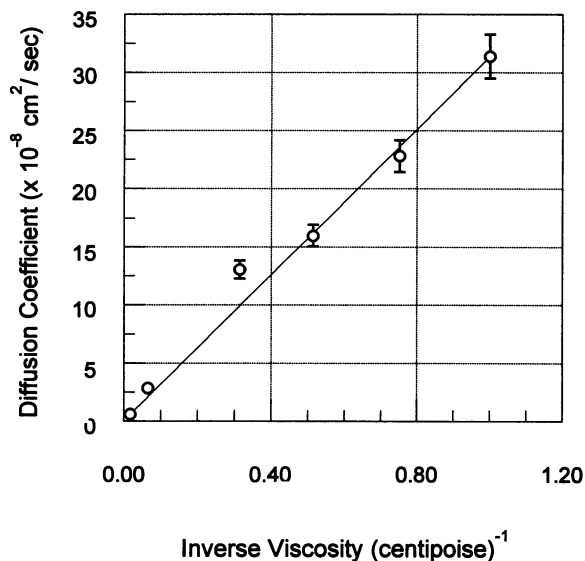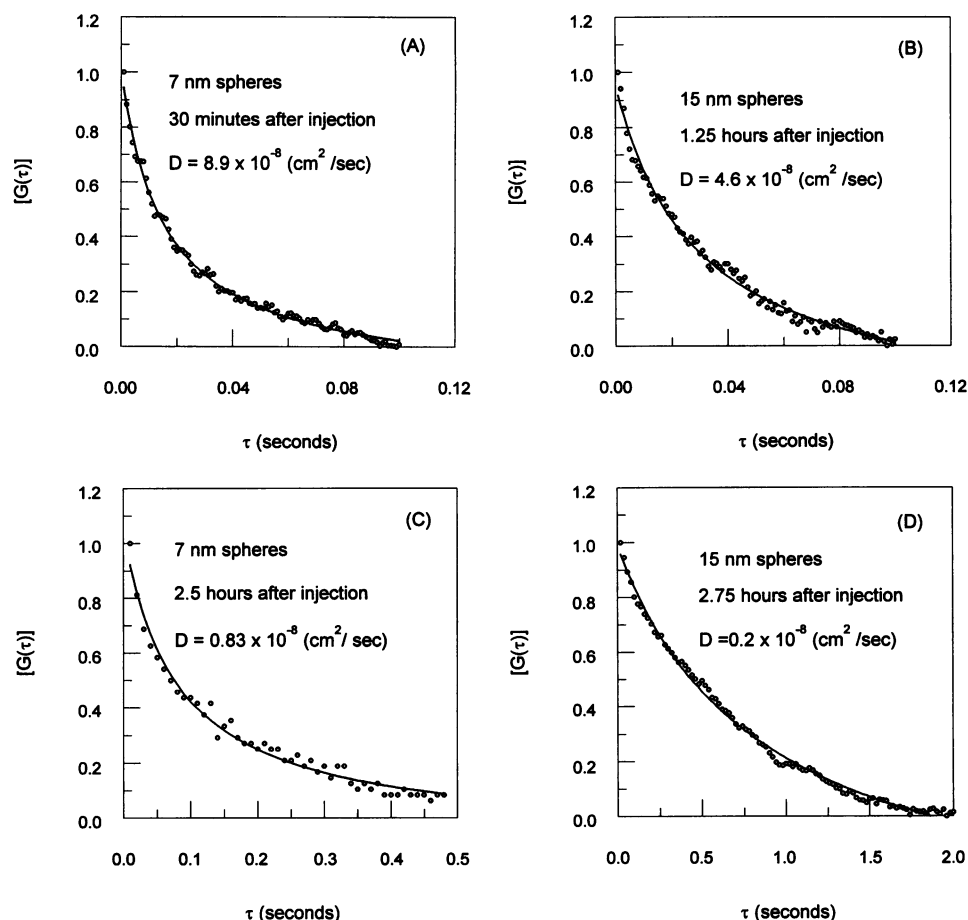

FIGURE 6   The diffusion coefficient for blue fluorescent spheres of 7 nm radius diffusing in solutions of multiple viscosity at 22°C. The solutions were sucrose water mixtures of 1.00, 1.33, 1.94, 3.18, 15.4, and 58.4 centipoise. The line shows the values of D expected according to Stokes-Einstein. Some error bars are smaller than the points plotted.

FIGURE 7 Measured autocorrelation functions for the diffusion of spheres in the cytoplasm of mouse fibroblast cells. $[G(\tau)]$ is the normalized $G(\tau)$ with the flat background subtracted. (A) 7-nm yellow-green fluorescent spheres diffusing 30 min after injection by electroporation. (B) 15-nm yellow-green fluorescent spheres diffusing 1 h and 15 min after electroporation. (C) 7-nm spheres diffusing 2 h and 30 min after electroporation. (D) 15-nm spheres diffusing 2 h and 45 min after electroporation.

have already been used in photobleaching recovery studies. It will be interesting to compare the results.

There are two major obstacles/limitations to doing FCS in a cell. The first problem is the autofluorescence of the cell, which is quite bright (Roederer and Murphy, 1986). The background signal contributed by the autofluorescence is a major problem, since for FCS we would like to use a probe at dilute concentration, 10–200 nM. The size of the background limits how much we can dilute the sample and still see the probe above the background. One way we were able to alleviate some of the problem was by moving to longer wavelength and exciting at 480 nm. The background still is a problem, but with bright probes like the spheres we could still make the measurements. At 960 nm excitation, it is possible that water absorption can cause local heating (absorption by the probe does not cause significant temperature variation). Measurements of the temperature changes in phospholipid vesicles illuminated with 1064-nm light (optical trapping) have shown temperature increases on the order of 1.1°C/100 mW (Liu et al., 1994). This is also a reasonable number for cellular systems (B. J. Tromberg, personal communication). Since we always use less than 10 mW at the sample for cellular studies (usually less than 1 mW), we should not see significant temperature increases due to water absorption. A second potential problem associated with the measurement is optical trapping. An optical trap is con-

structed simply by tightly focusing a laser on the sample, and we know that at certain laser power levels we can observe optical trapping of large particles in our system. At the powers used in these experiments, it is not possible to trap the 7-nm and 15-nm spheres used. Thus, the laser excitation may exert some forces on cellular components, and perhaps on the cell as a whole, but will not directly affect the motion of spheres unless they become large aggregates.

CONCLUSIONS

The main goal of this work was to demonstrate the possibility of investigating the properties of the intracellular environment using fluorescence correlation spectroscopy. We have demonstrated the benefits of two-photon fluorescence excitation for three dimensional FCS. These include automatic selection of a subvolume of a bulk sample, clear separation between excitation and emission wavelengths, and reduced photobleaching. We have reported accurate measurements of diffusion coefficients in bulk solution for many size fluorescent latex spheres, and at multiple viscosity. We then discussed the application of the method to cell interiors. We believe FCS has a lot of promise as a method to complement other studies of the cellular processes. In fact, in developing FCS to simultaneously monitor diffusion and aggregation or chemical reactions, it may be possible to make investigations

not yet possible with other methods. FCS is very sensitive. It is the extreme sensitivity of the method that makes it difficult to use with live systems, and thus it may not have the general applicability of photobleaching methods. On the other hand, for well designed experiments FCS has the potential to yield valuable insight into cellular structure and function, both in its own right, and by complementing results from other types of experiments. We are hopeful that future progress of this project can yield valuable information about the biology of the cell.

REFERENCES

Beckerle, M. C. 1984. Microinjected fluorescent polystyrene beads exhibit saltatory motion in tissue culture cells. *J. Cell Biol.* 98:2126–2132.

Bicknese, S., N. Periasamy, S. B. Shohet, and A. S. Verkman. 1993. Cytoplasmic viscosity near the cell plasma membrane: measurement by evanescent field frequency-domain microfluorimetry. *Biophys. J.* 65:1272–1282.

Borejdo, J. 1979. Motion of myosin fragments during actin-activated ATPase: fluorescence correlation spectroscopy study. *Biopolymers.* 18:2807–2820.

De Brabander, M., H. Geerts, R. Nuydens, and R. Nuyens. 1989. *Am. J. Anat.* 185:282–295.

Denk, W., J. H. Strickler, W. W. Webb. 1990. Two-photon laser scanning fluorescence microscopy. *Science.* 248:73–76.

Eigen, M., and R. Rigler. 1994. Sorting single molecules: application to diagnostics and evolutionary biotechnology. *Proc. Natl. Acad. Sci. USA.* 91:5740–5747.

Elson, E. L. 1985. Fluorescence correlation spectroscopy and photobleaching recovery. *Annu. Rev. Phys. Chem.* 36:379–406.

Elson, E. L., and D. Magde. 1974. Fluorescence correlation spectroscopy. I. Conceptual basis and theory. *Biopolymers.* 13:1–27.

Elson, E. L., D. Magde, and W. W. Webb. 1974. Fluorescence correlation spectroscopy. II. An experimental realization. *Biopolymers.* 13:29–61.

Fahey, P. F., and W. W. Webb. 1978. Lateral diffusion in phospholipid bilayer membranes and multilamellar liquid crystals. *Biochemistry.* 3046–3053.

Friedrich, D. M. 1982. Two-photon molecular spectroscopy. *J. Chem. Educ.* 59:472–481.

Icenogle, R. D., E. L. Elson. 1983a. Fluorescence correlation spectroscopy and photobleaching recovery of multiple binding reactions. I. Theory and FCS measurements. *Biopolymers.* 22:1919–1948.

Icenogle, R. D., E. L. Elson. 1983b. Fluorescence correlation spectroscopy and photobleaching recovery of multiple binding reactions. II. FPR and FCS measurements at low and high DNA concentrations. *Biopolymers.* 22:1919–1948.

Kao, H. P., J. R. Abney, and A. S. Verkman. 1993. Determinants of the translational mobility of a small solute in cell cytoplasm. *J. Cell Biol.* 120:175–184.

Kao, H. P., and A. S. Verkman. 1994. Tracking of single fluorescent particles in three dimensions: use of cylindrical optics to encode particle position. *Biophys. J.* 67:1291–1300.

Koppel, D. E., F. Morgan, A. Cowan, and J. H. Carson. 1994. Scanning concentration correlation spectroscopy using the confocal laser microscope. *Biophys. J.* 66:502–507.

Liu, Y., K. Cheng, G. J. Sonek, M. W. Berns, and B. J. Tromberg. 1994. *Appl. Phys. Lett.* 85:919–921.

Luby-Phelps, K. 1994. Physical properties of cytoplasm. *Curr. Opin. Cell Biol.* 6:3–9.

Luby-Phelps, K., Mujumdar, S., Mujumdar, R. B., Ernst, L. A., W. Galbraith, and A. Waggoner. 1993. A novel fluorescence radiometric method confirms the low solvent viscosity of the cytoplasm. *Biophys. J.* 65:236–242.

Luby-Phelps, K., D. L. Taylor, and R. Lanni. 1986. Probing the structure of cytoplasm. *J. Cell Biol.* 102:2015–2022.

Magde, M., W. W. Webb, and E. L. Elson. 1978. Fluorescence correlation spectroscopy. III. Uniform translation and laminar flow. *Biopolymers.* 17:361–376.

Meyer, T., and H. Schindler. 1988. Particle counting by fluorescence correlation spectroscopy: simultaneous measurement of aggregation and diffusion of molecules in solution and in membranes. *Biophys. J.* 54:983–993.

Palmer, A. G., and N. L. Thompson. 1987. Molecular aggregation characterized by high order autocorrelation in fluorescence correlation spectroscopy. *Biophys. J.* 52:257–270.

Petersen, N. O. 1984. Diffusion and aggregation in biological membranes. *Can. J. Biochem. Cell Biol.* 62:1158–1166.

Petersen, N. O. 1986. Scanning fluorescence correlation spectroscopy. I. Theory and simulation of aggregation measurements. *Biophys. J.* 49:809–815

Petersen, N. O., P. L. Hoddelius, P. W. Wiseman, O. Seger, and K. E. Magnusson. 1993. Quantitation of membrane receptor distributions by image correlation spectroscopy: concept and application. *Biophys. J.* 65: 1135–1146.

Petersen, N. O., D. C. Johnson, and M. J. Schlesinger. 1986. Scanning fluorescence correlation spectroscopy. II. Application to virus glycoprotein aggregation. *Biophys. J.* 49:809–815.

Piston, D. W., E.-S. Wu, and W. W. Webb. 1992. Three dimensional diffusion measurements in cells by two-photon excitation fluorescence photobleaching recovery. *Biophys. J.* 61:A34.

Qian, H., and E. L. Elson. 1990. Distribution of molecular aggregation by analysis of fluctuation moments. *Proc. Natl. Acad. Sci. USA.* 87: 5479–5483.

Qian, H., and E. L. Elson. 1991. Analysis of confocal laser-microscope optics for 3-D fluorescence correlation spectroscopy. *Appl. Optics.* 30: 1185–1195.

Rigler, R., U. Mets, J. Widengren, and P. Kask. 1993. Fluorescence correlation spectroscopy with high count rate and low background: analysis of translational diffusion. *Eur. Biophys. J.* 22:169–175.

Rigler, R., J. Widengren, and U. Mets. 1992. Interactions and kinetics of single molecules as observed by fluorescence correlation spectroscopy. *In* Fluorescence Spectroscopy: New Methods and Applications. I. S. Wolfbeis, editor. Springer, New York. 13–24.

St-Pierre, P. R., and N. O. Petersen. 1990. Relative ligand binding to small or large aggregates measured by scanning correlation spectroscopy. *Biophys. J.* 58:503–511.

Thompson, N. L. 1991. Fluorescence correlation spectroscopy. *In* Topics in Fluorescence Spectroscopy, Vol. 1: Techniques. J. R. Lakowicz, editor. Plenum, New York.

Wadsworth, P. 1987. Microinjected carboxylated beads move predominantly poleward in sea urchin eggs. *Cell Motil. Cytoskel.* 8:293–301.

Weissman, M., H. Schindler, and G. Feher. 1976. Determination of molecular weights by fluctuation spectroscopy: Application to DNA. *Proc. Natl. Acad. Sci. USA.* 73:2776–2780.